Cell Reports, Volume *30*

Supplemental Information

Memory B Cell Activation, Broad Anti-influenza Antibodies, and Bystander Activation Revealed by Single-Cell Transcriptomics

Felix Horns, Cornelia L. Dekker, and Stephen R. Quake

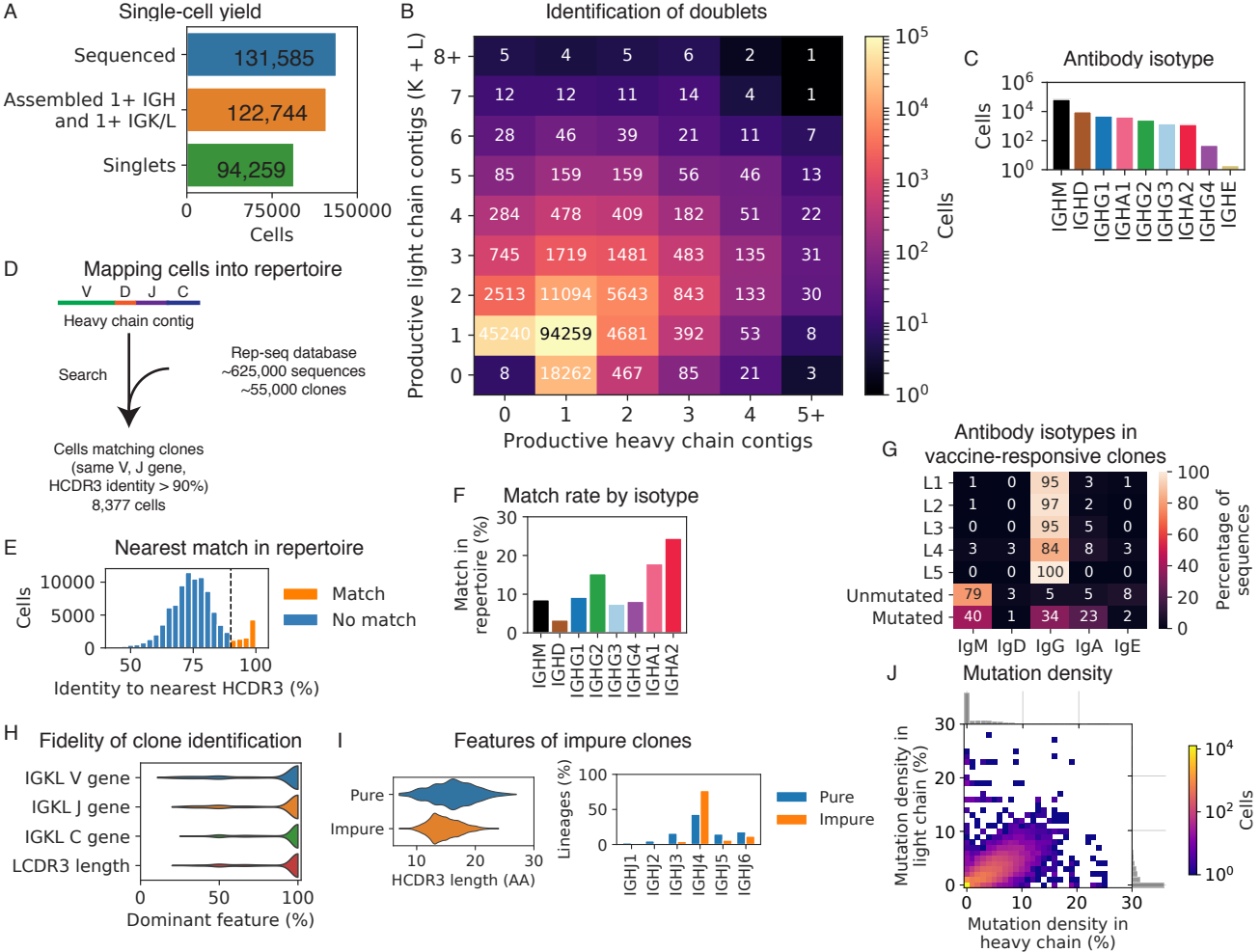
A
Single-cell yield
Sequenced
131,585
Assembled 1+ IGH and 1+ IGK/L
122,744
Singlets
94,259
0
75000
150000
Cells
B
Identification of doublets
Productive light chain contigs (K + L)
8+
7
6
5
4
3
2
1
0
5 4 5 6 2 1
12 12 11 14 4 1
28 46 39 21 11 7
85 159 159 56 46 13
284 478 409 182 51 22
745 1719 1481 483 135 31
2513 11094 5643 843 133 30
45240 94259 4681 392 53 8
8 18262 467 85 21 3
0 1 2 3 4 5+
Productive heavy chain contigs
Cells
10^5
10^4
10^3
10^2
10^1
10^0
C
Antibody isotype
Cells
10^6
10^4
10^2
10^0
IGHM
IGHD
IGHG1
IGHA1
IGHG2
IGHG3
IGHA2
IGHG4
IGHE
D
Mapping cells into repertoire
V D J C
Heavy chain contig
Search
Rep-seq database
~625,000 sequences
~55,000 clones
Cells matching clones
(same V, J gene,
HCDR3 identity > 90%)
8,377 cells
E
Nearest match in repertoire
Cells
10000
5000
0
50
75
100
Identity to nearest HCDR3 (%)
Match
No match
F
Match rate by isotype
Match in repertoire (%)
30
20
10
0
IGHM
IGHD
IGHG1
IGHG2
IGHG3
IGHG4
IGHA1
IGHA2
G
Antibody isotypes in vaccine-responsive clones
L1 1 0 95 3 1
L2 1 0 97 2 0
L3 0 0 95 5 0
L4 3 3 84 8 3
L5 0 0 100 0 0
Unmutated 79 3 5 5 8
Mutated 40 1 34 23 2
IgM IgD IgG IgA IgE
100
80
60
40
20
0
Percentage of sequences
H
Fidelity of clone identification
IGKL V gene
IGKL J gene
IGKL C gene
LCDR3 length
0
50
100
Dominant feature (%)
I
Features of impure clones
Pure
Impure
10
20
30
HCDR3 length (AA)
Lineages (%)
100
50
0
IGHJ1
IGHJ2
IGHJ3
IGHJ4
IGHJ5
IGHJ6
Pure
Impure
J
Mutation density
Mutation density in light chain (%)
30
20
10
0
0
10
20
30
Mutation density in heavy chain (%)
10^4
10^2
10^0
Cells

Figure S1. Performance and features of integrated single-cell and antibody repertoire sequencing measurements, Related to Figure 2.

(A) Number of single cells that were sequenced, had at least one productive heavy (IGH) and one light (IGK/L) chain gene assembled, or had exactly one productive heavy and one productive light chain gene assembled (singlets).

(B) Doublets were identified and removed based on the number of productive heavy and light chain contigs assembled. Heatmap shows the number of putative cells (cell barcodes) having the number of productive heavy and light chain (either kappa or lambda) contigs indicated by the x- and y-axis, respectively.

(C) Isotypes of antibodies from single B cells, as determined based on the heavy chain constant region sequence.

(D) Strategy for mapping single B cells to clones detected by repertoire sequencing using a custom search algorithm. Matches required usage of the same V and J genes and HCDR3 identity >90%.

(E) HCDR3 identity of nearest match in repertoire sequences. Dashed line indicates cutoff of 90% HCDR3 identity used for identification of bona fide matches.

(F) Isotypes of antibodies in the single cells that matched clones detected by repertoire sequencing (n = 8,377 cells)

(G) Isotypes of antibodies in vaccine-responsive clones, or in the mutated (V gene identity to germline < 100%) or unmutated (V gene identity to germline = 100%) fractions of the repertoire.

(H) Fidelity of clone identification was determined by assessing the fraction of single cells sharing the characteristics of the dominant light chain gene found within the clone.

(I) Molecular features of pure and impure clones (as determined based on light chain characteristics).

(J) Mutation density in the natively paired heavy and light chain genes of individual cells based on comparison with germline V gene. Marginal plots show univariate distributions of mutation density in each chain.

AA, amino acids; HCDR3, heavy chain complementarity determining region 3; LCDR3, light chain complementarity determining region 3.

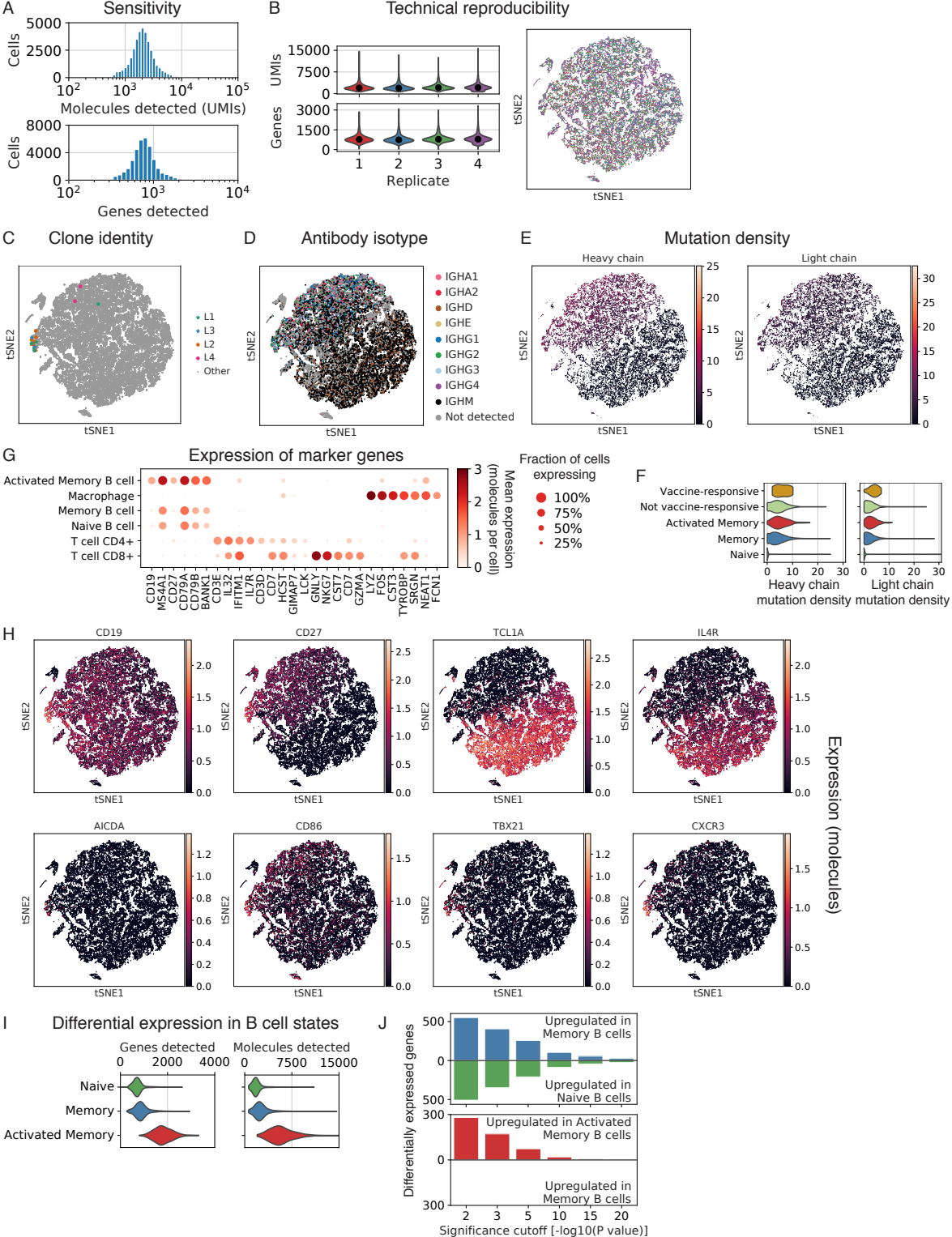
A
Sensitivity
Cells
5000
2500
0
10^2
10^3
10^4
10^5
Molecules detected (UMIs)
8000
4000
0
10^2
10^3
10^4
Genes detected
B
Technical reproducibility
UMIs
15000
7500
0
Genes
3000
1500
0
1
2
3
4
Replicate
tSNE2
tSNE1
C
Clone identity
L1
L3
L2
L4
Other
D
Antibody isotype
IGHA1
IGHA2
IGHD
IGHE
IGHG1
IGHG2
IGHG3
IGHG4
IGHM
Not detected
E
Mutation density
Heavy chain
Light chain
G
Expression of marker genes
Activated Memory B cell
Macrophage
Memory B cell
Naive B cell
T cell CD4+
T cell CD8+
CD19
MS4A1
CD27
CD79A
CD79B
BANK1
CD3E
IL32
IFITM1
IL7R
CD3D
CD7
HCST
GIMAP7
LCK
GNLY
NKG7
CST7
CD7
GZMA
LYZ
FOS
CST3
TYROBP
SRGN
NEAT1
FCN1
Mean expression (molecules per cell)
Fraction of cells expressing
100%
75%
50%
25%
F
Vaccine-responsive
Not vaccine-responsive
Activated Memory
Memory
Naive
Heavy chain mutation density
Light chain mutation density
H
CD19
CD27
TCL1A
IL4R
AICDA
CD86
TBX21
CXCR3
Expression (molecules)
I
Differential expression in B cell states
Genes detected
Molecules detected
Naive
Memory
Activated Memory
J
Upregulated in Memory B cells
Upregulated in Naive B cells
Upregulated in Activated Memory B cells
Upregulated in Memory B cells
Differentially expressed genes
Significance cutoff [-log10(P value)]

Figure S2. Additional characterization of transcriptional profiles, clonal origins, and molecular features of antibodies in single cells isolated from peripheral blood after influenza vaccination, Related to Figure 3.

(A) Genes and molecules detected in each individual cell. UMIs, unique molecular identifiers.

(B) Reproducibility in technical replicates. Left panel shows distributions of genes and molecules detected in individual cells in different technical replicates. Median is indicated by black dot. Right panel shows the transcriptome profiles of individual cells, visualized using principal components analysis (PCA) and t-distributed Stochastic Neighbor Embedding (tSNE) as in Figure 3. Each dot is a cell colored by technical replicate of origin, according to the colors in left plots.

(C–E) Clonal origin and molecular features of individual cells. Cells are visualized as in Figure 3 and colored by clone identity as revealed by Rep-seq (C), antibody isotype (D), or density of somatic mutations in the V gene in comparison with germline (E), as revealed by single-cell heavy chain assembly (D and E). In (C), vaccine-responsive clones that bind vaccine (L1 and L3) or do not bind vaccine (L2 and L4) are indicated by stars or circles, respectively. L5 is not shown because gene expression information was not obtained for any cells belonging to this clone.

(F) Density of somatic mutations in the V gene of the heavy chain (left) or light chain (right) in comparison to the germline for single cells annotated based on dynamics (vaccine-responsive or not vaccine-responsive) or gene expression profile (activated memory, memory, or naïve B cells).

(G) Expression of established marker genes in clusters. Clusters were manually annotated based on these expression profiles.

(H) Expression of selected established marker genes and genes of immunological interest in single cells. Cells are visualized as in Figure 3 and colored by expression of the gene indicated by the title of the plot.

(I) Distributions of genes and molecules detected in B cells in distinct states.

(J) Differential expression analysis identified genes upregulated in naïve compared to memory B cells (green), memory compared naïve B cells (blue), and activated memory compared to memory B cells (red) across a range of significance cutoffs.

A

Features of vaccine-responsive antibody clones

Clone	Antibodies produced	Antibodies sequenced	Abundance at D7 (%)	FC D0 to D7	HV gene	HJ gene	HCDR3 length (AA)	LV gene	LJ gene	LCDR3 length (AA)
L1	5	48	8.5	4360	V3-15*01	J5*02	16	LV6-57	LJ2	12
L2	5	40	6.7	∞	V4-59*08	J4*02	17	LV2-23	LJ3	12
L3	7	7	0.2	∞	V4-34*01	J3*01	19	KV1-39	KJ3	5
L4	3	3	0.1	62	V1-3*01	J6*03	20	KV3-20	KJ3	9
L5	1	1	0.1	∞	V4-59*08	J4*02	19	LV2-23	LJ3	11

B

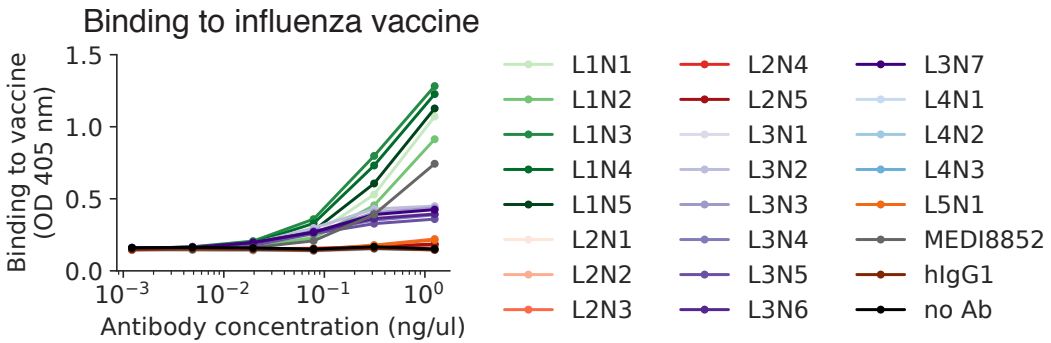

C

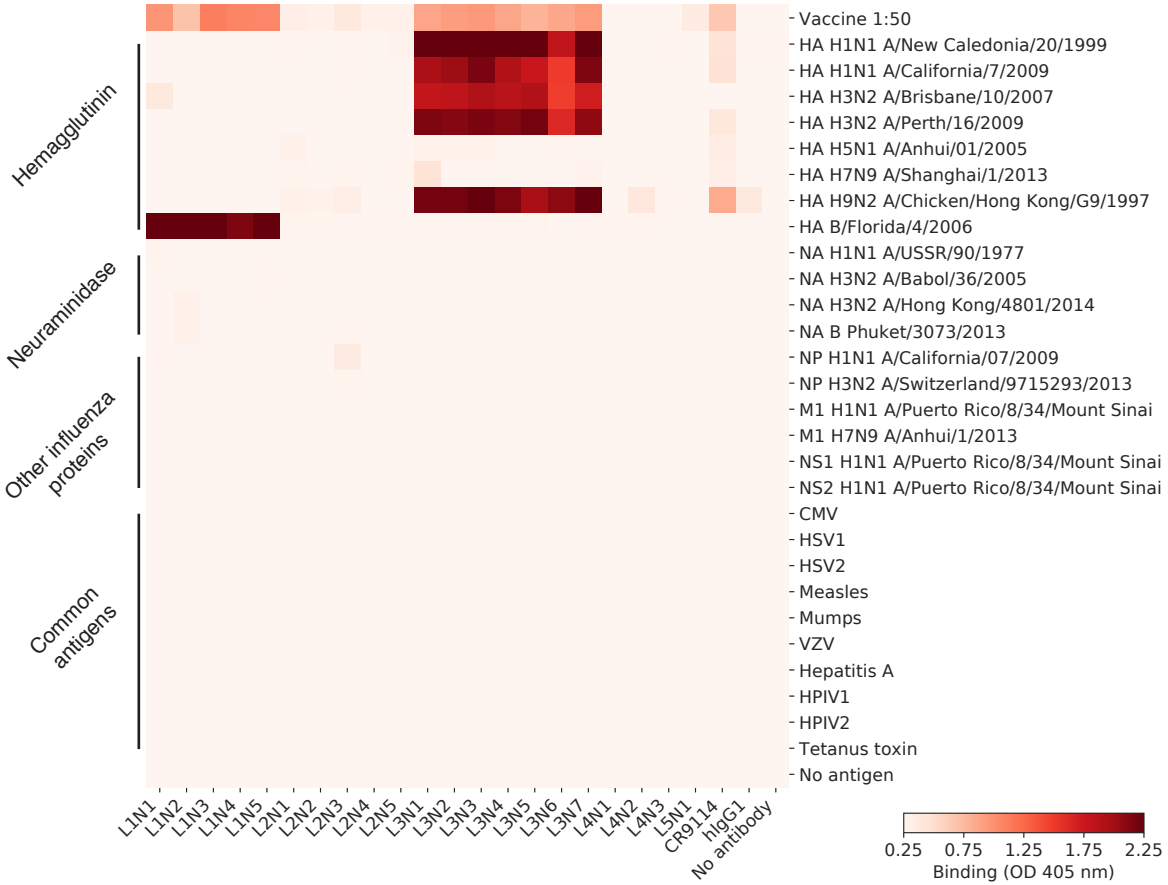

Figure S3. Molecular features and functional characterization of influenza vaccine-responsive antibodies, Related to Figure 4.

(A) Molecular features and population dynamics of vaccine-responsive antibody clones. "Antibodies sequenced" indicates the number of cells captured by droplet-based single-cell sequencing, and thus antibodies having native heavy and light chain sequences. FC, fold-change; D0, day 0 after vaccination; D7, day 7 after vaccination; AA, amino acids.

(B and C) Binding of vaccine-responsive antibodies to the vaccine given to the subject (trivalent inactivated influenza vaccine from the 2011–2012 flu season) (B) and to purified influenza proteins and common viral and bacterial antigens (C) was measured using enzyme-linked immunosorbent assay (ELISA).

HA, hemagglutinin; NA, neuraminidase; NP, nucleoprotein, M1, matrix protein 1; NS1, non-structural protein 1; NS2, non-structural protein 2; CMV, cytomegalovirus; HSV1/2, herpes simplex virus 1/2; VZV, varicella zoster virus; HPIV1/2, human parainfluenza virus 1/2; OD, optical density; hIgG1, human IgG1; no Ab, no antibody.

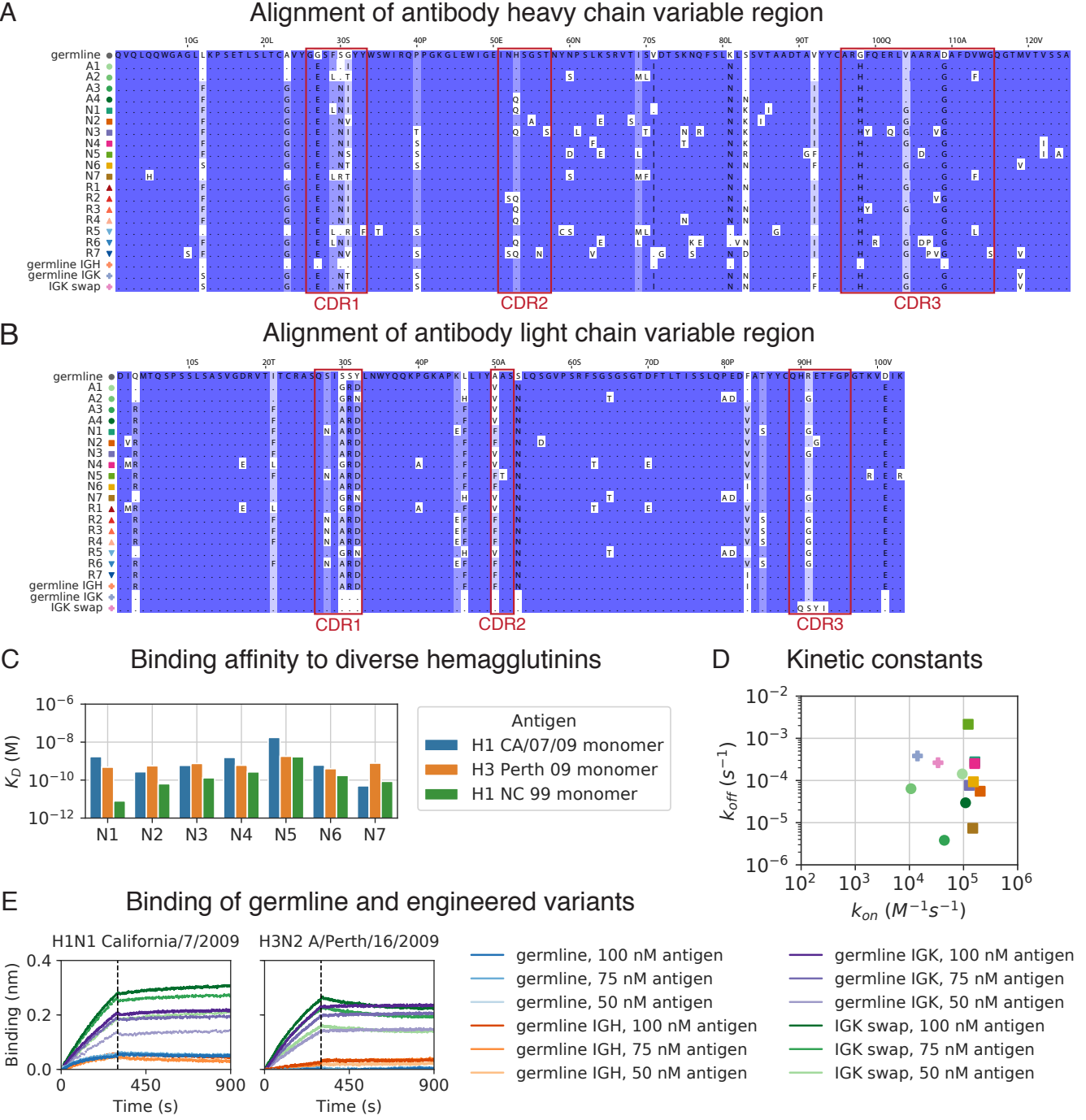
A
Alignment of antibody heavy chain variable region
germline
A1
A2
A3
A4
N1
N2
N3
N4
N5
N6
N7
R1
R2
R3
R4
R5
R6
R7
germline IGH
germline IGK
IGK swap
CDR1
CDR2
CDR3
B
Alignment of antibody light chain variable region
CDR1
CDR2
CDR3
C
Binding affinity to diverse hemagglutinins
K_D (M)
N1
N2
N3
N4
N5
N6
N7
Antigen
H1 CA/07/09 monomer
H3 Perth 09 monomer
H1 NC 99 monomer
D
Kinetic constants
k_{off} (s^{-1})
k_{on} ($M^{-1}s^{-1}$)
E
Binding of germline and engineered variants
H1N1 California/7/2009
H3N2 A/Perth/16/2009
Binding (nm)
Time (s)
germline, 100 nM antigen
germline, 75 nM antigen
germline, 50 nM antigen
germline IGH, 100 nM antigen
germline IGH, 75 nM antigen
germline IGH, 50 nM antigen
germline IGK, 100 nM antigen
germline IGK, 75 nM antigen
germline IGK, 50 nM antigen
IGK swap, 100 nM antigen
IGK swap, 75 nM antigen
IGK swap, 50 nM antigen

Figure S4. Molecular features and functional characterization of a broadly binding anti-influenza antibody clone, Related to Figure 5.

(A and B) Alignments of heavy (A) and light (B) chain variable region protein sequences for antibodies and engineered variants from clone L3. As in Figure 5, these antibodies include extant sequences (N1–7), reconstructed ancestral sequences (germline and A1–4), and engineered variants having the L3N6 sequences, but with heavy chain reverted to the inferred germline sequence (germline IGH), light chain reverted to the inferred germline sequence (germline IGK), or a light chain sequence substituted from a different clone (IGK swap). Germline genes were *HV4-34*01*, *HJ3*01*, *KV1-39*, and *KJ3*. CDRs are indicated by red boxes. Background color indicates conservation of the position. Residues that are the same as germline are indicated by ".".

(C and D) Equilibrium constants (K_D) (C) and kinetic constants (k_{on} and k_{off}) (D) of binding between antibody variants from L3 and hemagglutinin variants were measured using biolayer interferometry. Symbols denoting variants are shown in Figure S4A.

(E) Kinetics of binding and unbinding of germline and engineered antibody variants to H1 (A/California/7/2009) (left) and H3 (A/Perth/16/2009) (right) hemagglutinin antigens. Colors indicate antibody variants and antigen concentration. Dashed line indicates transition from association to dissociation step. Note that determination of equilibrium binding constants (shown in Figure 5C) was performed at lower antigen concentrations (not shown here).

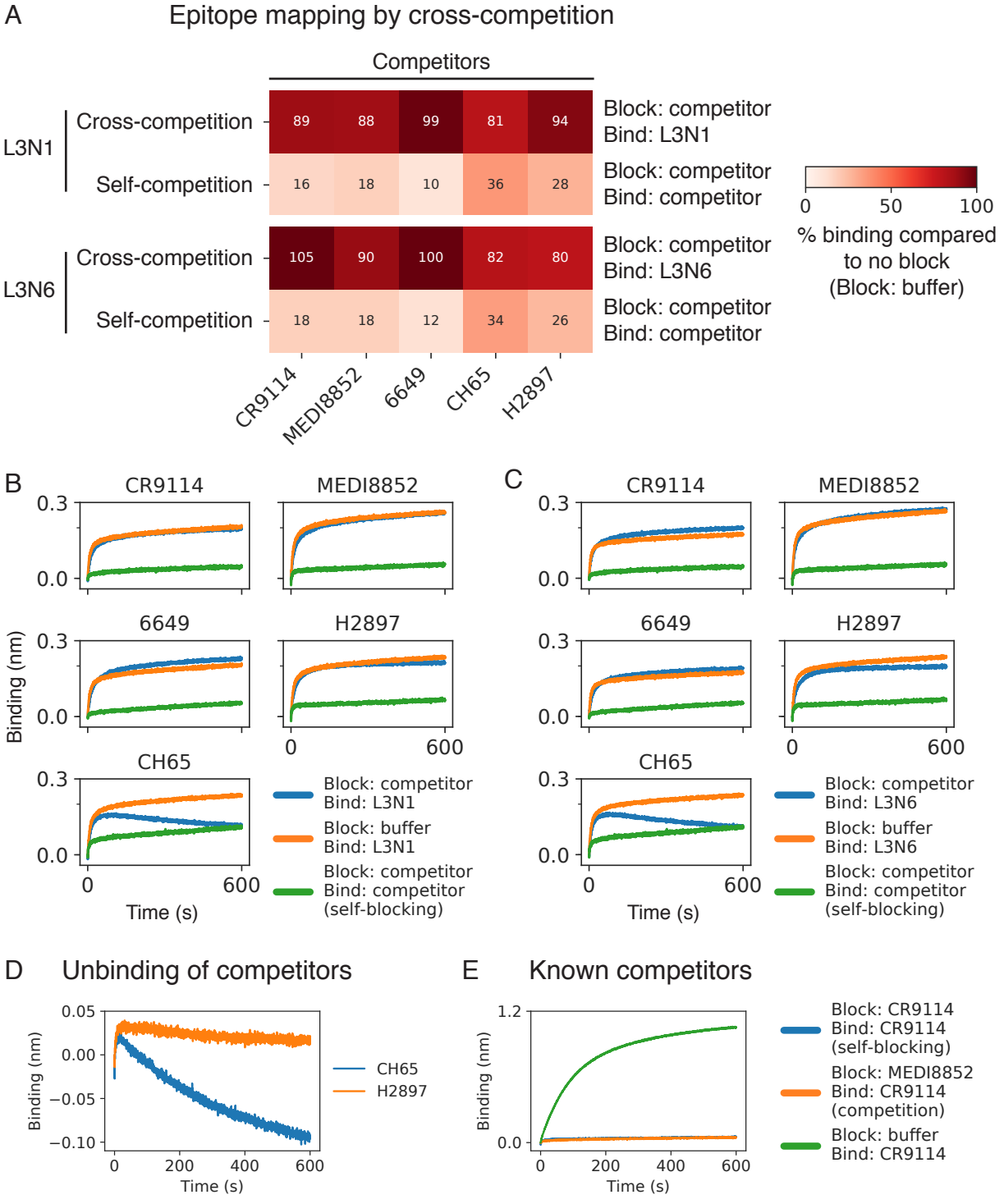
A
Epitope mapping by cross-competition
Competitors
L3N1
Cross-competition
Self-competition
L3N6
Cross-competition
Self-competition
89 88 99 81 94
16 18 10 36 28
105 90 100 82 80
18 18 12 34 26
Block: competitor
Bind: L3N1
Block: competitor
Bind: competitor
Block: competitor
Bind: L3N6
Block: competitor
Bind: competitor
0
50
100
% binding compared
to no block
(Block: buffer)
CR9114
MEDI8852
6649
CH65
H2897
B
C
CR9114
MEDI8852
6649
H2897
CH65
0.3
0.0
Binding (nm)
0
600
Time (s)
Block: competitor
Bind: L3N1
Block: buffer
Bind: L3N1
Block: competitor
Bind: competitor
(self-blocking)
Block: competitor
Bind: L3N6
Block: buffer
Bind: L3N6
Block: competitor
Bind: competitor
(self-blocking)
D
Unbinding of competitors
0.05
0.00
−0.05
−0.10
Binding (nm)
0
200
400
600
Time (s)
CH65
H2897
E
Known competitors
1.2
0.0
Binding (nm)
0
200
400
600
Time (s)
Block: CR9114
Bind: CR9114
(self-blocking)
Block: MEDI8852
Bind: CR9114
(competition)
Block: buffer
Bind: CR9114

Figure S5. Determination of antibody epitopes by cross-competition, Related to Figure 5.
(A–C) Binding of antibodies L3N1 and L3N6 to trimeric hemagglutinin (H1 A/New Caledonia/20/1999) following blocking with potentially competing antibodies as determined by biolayer interferometry.
In (B) and (C), the kinetics of binding of L3N1 (B) and L3N6 (C) are shown, after blocking with the competitor indicated by the title of each subpanel. To summarize these data (A), binding was determined after 50 s and compared with binding observed in the absence of blocking (i.e., using buffer instead of a potentially competing antibody during the blocking step).
(D) Kinetics of unbinding for competitors CH65 and H2897. Fast unbinding of CH65 explains the observed decrease in binding in (B) and (C).
(E) Kinetics of binding of CR9114 to trimeric hemagglutinin (H1 A/New Caledonia/20/1999) following blocking with MEDI8852. Blue indicates self-blocking (block with CR9114, followed by binding of CR9114), while orange indicates competition (block with MEDI8852, followed by binding of CR9114); blue is almost entirely hidden behind orange. Green indicates absence of blocking (block with buffer, followed by binding of CR9114). CR9114 and MEDI8852 have overlapping epitopes, as determined by crystal structures; therefore, the observed competition is expected.